



THE UNIVERSITY *of* EDINBURGH

Edinburgh Research Explorer

An Orally Active Galectin-3 Antagonist Inhibits Lung Adenocarcinoma Growth and Augments Response to PD-L1 Blockade

Citation for published version:

Vuong, L, Kouverianou, E, Rooney, CM, McHugh, BJ, Howie, SEM, Gregory, CD, Forbes, SJ, Henderson, NC, Zetterberg, FR, Nilsson, UJ, Leffler, H, Ford, P, Pedersen, A, Gravelle, L, Tantawi, S, Schambye, H, Sethi, T & MacKinnon, AC 2019, 'An Orally Active Galectin-3 Antagonist Inhibits Lung Adenocarcinoma Growth and Augments Response to PD-L1 Blockade', *Cancer Research*, vol. 79, no. 7, pp. 1480-1492. <https://doi.org/10.1158/0008-5472.CAN-18-2244>

Digital Object Identifier (DOI):

[10.1158/0008-5472.CAN-18-2244](https://doi.org/10.1158/0008-5472.CAN-18-2244)

Link:

[Link to publication record in Edinburgh Research Explorer](#)

Document Version:

Peer reviewed version

Published In:

Cancer Research

Publisher Rights Statement:

This is the author's peer reviewed version as accepted for publication.

General rights

Copyright for the publications made accessible via the Edinburgh Research Explorer is retained by the author(s) and / or other copyright owners and it is a condition of accessing these publications that users recognise and abide by the legal requirements associated with these rights.

Take down policy

The University of Edinburgh has made every reasonable effort to ensure that Edinburgh Research Explorer content complies with UK legislation. If you believe that the public display of this file breaches copyright please contact openaccess@ed.ac.uk providing details, and we will remove access to the work immediately and investigate your claim.



A Novel, Orally Active Galectin-3 Antagonist Inhibits Lung Adenocarcinoma Growth and Augments Response to PD-L1 Blockade

Lynda Vuong², Eleni Kouverianou¹, Claire M. Rooney², Brian J. McHugh¹, Sarah E.M. Howie¹, Christopher Gregory¹, Stuart J. Forbes³, Neil C. Henderson¹, Fredrik Zetterberg⁴, Ulf J Nilsson⁵, Hakon Leffler⁶, Paul Ford⁴, Anders Pedersen⁴, Lise Gravelle⁴, Susan Tantawi⁴, Hans Schambye⁴, Tariq Sethi^{2†} Alison C. MacKinnon^{1†}

Affiliations:

¹University of Edinburgh, Centre for Inflammation Research, Queen's Medical Research Institute, Edinburgh Bioquarter, 47 Little France Crescent, Edinburgh EH16 4TJ, UK.

²Department of Asthma, Allergy and Respiratory Science, King's College London, Guy's hospital, London SE1 9RT, UK.

³MRC Centre for Regenerative Medicine, University of Edinburgh, Edinburgh Bioquarter, 5 Little France Drive, Edinburgh EH16 4UU, UK.

⁴Galecto Biotech, Cobis Science Park, Ole Maaloes Vej 3, DK-2200 Copenhagen, Denmark.

⁵Centre for Analysis and Synthesis, Department of Chemistry, Lund University, POB 124, SE-221 00 Lund, Sweden.

⁶Department of Laboratory Medicine, Section MIG, Lund University, BMC-C1228b, Klinikgatan 28, SE-221 84 Lund, Sweden

[†]These authors contributed equally

Running title: Novel galectin-3 antagonist inhibits lung cancer progression

Keywords: Galectin-3, Lung Cancer, Macrophages, Immune checkpoint inhibitors, T cells

Funding: The work presented was funded by Galecto Biotech, a King's Health School's scholarship to L.V. and a Norman Salvesen Emphysema Research grant to E.K.

Correspondence: A.Mackinnon@ed.ac.uk, Phone: 0044 131 242 6685, Fax: 0044 131 242 6578

Conflicts of interest:

This work was supported in part by Galecto Biotech. L.V., B.M. and A.C.M. are supported in part by Galecto Biotech, F.Z., P.F., A.P., L.G., S.T. and H.S. are employees and shareholders of Galecto Biotech; H.S., T.S., U.J.N., H.L are founders and shareholders of Galecto Biotech and are members of its scientific advisory board.

Word Count: 4998

Total number of figures: 5

Precis:

A novel and orally active galectin-3 antagonist inhibits lung adenocarcinoma growth and metastasis and augments response to PD-L1 blockade.

Abstract:

A combination therapy approach is required to improve tumor immune infiltration and patient response to immune checkpoint inhibitors targeting negative regulatory receptors. Galectin-3 is a β -galactoside-binding lectin highly expressed within the tumor microenvironment of high fatality cancers and its expression correlates particularly with poor survival in non-small cell lung cancer (NSCLC) patients. To examine the role of galectin-3 inhibition in NSCLC we tested the effects of galectin-3 depletion using genetic and pharmacological approaches on syngeneic mouse lung adenocarcinoma and human lung adenocarcinoma xenografts. We show that galectin-3^{-/-} mice develop significantly smaller and fewer tumors and metastases than syngeneic C57/Bl6 wild type mice. We demonstrate that macrophages are a major driver of this response as macrophage ablation retards tumor growth whilst reconstitution with galectin-3 positive bone marrow restores tumor growth in galectin-3^{-/-} mice. Oral administration of a novel small molecule galectin-3 inhibitor GB1107 reduces human and mouse lung adenocarcinoma growth and blocks metastasis in the syngeneic model. Treatment with GB1107 increases tumor M1 macrophage polarization and CD8⁺ cell infiltration. Moreover, it potentiates the effects of a PD-L1 immune checkpoint inhibitor, to increase expression of cytotoxic (IFN- γ , granzyme B, perforin-1, fas ligand) and apoptotic (cleaved caspase-3) effector molecules. Galectin-3 is an important regulator of lung adenocarcinoma progression. A novel galectin-3 inhibitor could provide effective non-toxic monotherapy treatment as well as in combination, boost immune-infiltration and responses to current immune checkpoint inhibitors in lung adenocarcinoma and potentially other high fatality cancers.

Introduction

Globally, lung cancer is the leading cause of cancer-related mortality (1). Non-small cell lung carcinoma (NSCLC) comprises 80% of total lung cancer cases, with lung adenocarcinoma being the major subtype (1). In recent years immune checkpoint therapies targeting various negative regulatory receptors on tumor infiltrating cytotoxic T lymphocytes (CTLs) such as Programmed Death-1 (PD-1), Programmed Death-Ligand 1 (PD-L1), Cytotoxic T-Lymphocyte Associated Protein 4 (CTLA-4) and others, have shown unprecedented efficacy in NSCLC patients even against late stage disease (2). However patient response is limited, thus driving intensive research toward combining immune checkpoint inhibition with other targeted agents to overcome resistance (2).

Tumor-associated macrophages (TAMs) are present in the stroma of many tumors including NSCLC (3). TAMs acquire an alternative (M2)-like macrophage phenotype and secrete angiogenic and anti-inflammatory cytokines, which contribute to the immunosuppressive milieu of the tumor microenvironment (4). TAMs can also be important direct targets of PD-1/PD-L1 inhibition and can also promote drug resistance by removing anti-PD-1 antibodies from T cells (5, 6). Indeed, macrophage depletion via colony-stimulating factor-1 receptor (CSF-1R) blockade improved T cell infiltration and antitumor activity of PD-1 antagonists in preclinical models of melanoma and breast cancer (7, 8), suggesting that strategies aimed at inhibiting macrophage responses are necessary to permit effective immune checkpoint therapy.

One possible target for such combination treatment is galectin-3, a member of a protein family defined by affinity for β -galactoside-containing glycoconjugates and a conserved carbohydrate-recognition-binding domain (CRD) (9). Galectin-3 is widely expressed in several cell types such as macrophages, fibroblasts, activated T-lymphocytes and epithelial cells (10-12) and is highly expressed in high fatality cancers such as NSCLC (13). In NSCLC particularly in adenocarcinoma, increased galectin-3 expression in tumors, lymph nodes and serum correlates with metastases and is a negative prognostic indicator (13-18). The galectin-3 genetic polymorphism rs4652 associated with impaired galectin-3 secretion, has been linked to increased survival and response to chemotherapy in NSCLC (18). Galectin-3 can directly enhance cell proliferation (19), apoptosis resistance (20), metastatic potential (19, 21), as well as lung cancer stemness (22). It is also an important constituent of the tumor microenvironment acting on endothelial cells to promote angiogenesis (23). Furthermore many studies have revealed the inhibitory effects of galectin-3 on activated cytotoxic T lymphocytes CTLs (24-27) and we have shown it to be essential for M2 macrophage differentiation (28, 29). Hence, galectin-3 forms an ideal candidate target for combining with checkpoint blockade.

We examined the role of galectin-3 in NSCLC by utilizing the syngeneic mouse Lewis Lung Carcinoma (LLC1) model, comparing tumor growth in wild-type and galectin-3-deficient mice showing an essential non-redundant tumor-promoting role for galectin-3. Bone marrow transfer and macrophage depletion experiments show that macrophages are a major source of tumor promoting galectin-3. A newly developed, selective small molecule galectin-3 inhibitor inhibited mouse and human NSCLC tumor growth and metastasis and significantly potentiated response to an immune checkpoint blockade.

Materials and Methods

Cell Lines, Culture and Transfections

LLC1 cells and A549 cells were purchased from the European Cell Culture Collection (ECACC 90020104) and were cultured at 37°C in 5% CO₂ (95% air) in Dulbecco's modified Eagles medium (Sigma D5671) supplemented with 10% fetal calf serum (FCS), 1% L-glutamine and 1% penicillin/streptomycin. Vector pCMV-KDEL-Gluc-1, expressing G.princeps luciferase (Lux Biotechnologies) was transfected by electroporation (Lonza electroporation kit VCO-1001). Stably transfected cells were selected with G418. LLC1-luciferase cells were transduced with lentiviral particles packaged in H293T cells containing either non-targeting control shRNA or a mouse galectin-3 targeting shRNA (G501) within a pGIPZ vector (GE Dharmacon). Successfully transduced cells were selected in 3µg/ml of puromycin for 10 days followed by flow sorting for GFP⁺ cells using a BD FACS-Aria.

Animals

All animal experimental work was carried out according to UK Home Office Guidelines (Animals (Scientific Procedures) Act 1986). C57Bl/6 mice and female CD1 nude mice were purchased from Harlan Laboratories. Generation of galectin-3^{-/-} mice by gene-targeting technology has been described previously (30). CD11b-DTR (Diphtheria Toxin Receptor) mice were derived from FVB mice as described (31) and backcrossed over 10 generations onto the C57Bl/6 background. Human galectin-3 knockin mice were generated by Cyagen Biosciences using the TurboKnockout (conditional Knockin) approach by inserting the entire

human LGALS3 sequence into exon 1 of mouse Lgals3 so that the expression of human galectin-3 is under control of the mouse gene regulatory element.

Orthotopic LLC1 model

Mice were anaesthetized with isofluorane. A 1mm skin incision was made below the right shoulder blade. 10^3 LLC1 cells stably expressing Gaussia luciferase (see supplemental information) were injected through the intercostal muscles into the lung parenchyma prior to the incision being stapled.

Subcutaneous LLC1 model

LLC1 (2.5×10^5) cells were injected subcutaneously into the flanks of age-matched male wild type and galectin-3^{-/-} C57Bl/6 mice. Each animal received an injection of 2.5×10^5 cells suspended in 100 μ L PBS in both flanks. Tumor volumes were measured with callipers every 1-3 days (tumor volume = $\pi/6 \times (L \times W)^{3/2}$).

LLC1 metastasis model

LLC1 cells were administered via the tail vein (1×10^6 cells) and lungs harvested at 7 days. RNA was extracted from whole lungs using a Qiagen RNeasy kit, converted into cDNA (Quantitect cDNA synthesis kit; Qiagen) and luciferase expression was measured by qPCR using primers against Gaussia princeps luciferase (5'-TCTGCCTGTCCCACATCAAG-3' forward and 3'-CCCTGTGCGGACTCTTTGT-5' reverse; Primer Design) and SYBR Green (ThermoFisher Scientific).

Human adenocarcinoma xenograft model

CD-1 nude female mice received 3×10^6 human lung adenocarcinoma cells (A549) in 100 μ l 1:1 matrigel:serum free DMEM in both flanks. Tumor volumes were measured every 2-3 days using digital calipers.

Macrophage ablation

Macrophages were ablated in C57Bl/6 CD11b-DTR mice (or WT littermates) by administration of 10ng/g diphtheria toxin (DT) intraperitoneally (I.P.) prior to subcutaneous tumor cell injections.

Bone Marrow transplant

Mice were injected with 400 μ L liposomal clodronate (Liposoma). After 36h mice were irradiated with 10.5 Gy delivered from an IBL637 gamma irradiator (Gamma Services Ltd) at a dose-rate of 0.64 Gy/min. Following irradiation mice received a single tail-vein infusion of 10^7 bone marrow cells obtained by flushing the femurs of WT and galectin-3^{-/-} donor mice. Transplanted mice were used 8 weeks post-transplant.

Drug preparation

Galectin-3 inhibitor GB1107 (3,4-dichlorophenyl 3-deoxy-3-[4(3,4,5-trifluorophenyl)-1H-1,2,3-triazol-1-yl]-1-thio- α -D-galactopyranoside; Galecto Biotech; Copenhagen, Denmark (32)) was prepared at a concentration of 1mg/ml in 1% polyethylene glycol, 0.5% hydroxypropyl methyl cellulose (HPMC) and stored in aliquots at -20°C. The anti-PD-L1 monoclonal antibody (clone 10F.9G2) used for *in vivo* blockade experiments was purchased from BioXCell and 200 μ g in

PBS was administered twice weekly by I.P. injection.

Luciferase Assays

LLC1 cells stably transfected with pCMV-KDEL-Gluc-1 were assessed for luciferase expression upon addition of n-colenterazine (n-CTZ) (Lux Biotechnologies 20001) substrate to a final concentration of 10 μ M to live cells in 96-well plates. Lymph nodes were disaggregated by passing through 40 μ m cell strainers and suspended in PBS. N-CTZ was added at a final concentration of 10 μ M. Luciferase activity was assessed with a BioTek SynergyTM HT Luminometer.

Immunohistochemistry

Formalin fixed paraffin embedded sections were deparaffinized in xylene and rehydrated in graded ethanol. Epitopes were retrieved by microwaving in 0.01M sodium citrate (pH 6) for Ym1, and ki-67 staining and by proteinase K digest (1.25 mg/mL) for 5 min for F4/80 staining. Sections were blocked with serum-free protein block (DAKO) and incubated overnight at 4°C with primary antibodies, rabbit anti-mouse Ym1 (Stem Cell Technologies, 1:200), rat anti-mouse F4/80 (Abcam, 1:100), rabbit anti-mouse ki-67 (Abcam, 1:200) and rabbit anti-mouse cleaved caspase-3 (clone 5A1, Abcam, 1:1000). Sections were incubated with species-specific biotinylated IgG (Vector), and visualized with 3,3'-diaminobenzidine (DAB) substrate.

Immunohistochemistry Quantifications

Five to ten fields were scored for each tumor representing both tumor and stroma. Absolute cell counts were recorded for F4/80 and Ym1 positive cells. Ki-67 positive nuclei were counted in whole tumors from slide scans using Image J. and presented as a ratio of Ki-67⁺ nuclei/total nuclei. Cleaved caspase-3 staining in tumors was quantified by inverting 8-bit TIFF files so that DAB-positive areas give the highest pixel intensities. Mean pixel intensities (MPI) were then measured in up to 160 fields of view covering the entire tumor parenchyma and averaged to give a single value per tumor. F4/80 was quantified using Image J by selecting brown DAB⁺ areas using color thresholding (hue 0-128, saturation 0-255, brightness 0-170), inverting 8-bit TIFF files and measuring MPI.

Immunofluorescence

LLC1 cells were plated on coverslips and stained for galectin-3 with FITC conjugated rat anti-mouse galectin-3 (1:200; clone CL8942F; Cedarlane) and Alexa Fluor 488-conjugated donkey anti-rat secondary antibody (1:500; clone A21208; Invitrogen) before or after permeabilisation with 0.2% Triton X-100 in PBS for 10mins. Cells were counterstained with DAPI and mounted in Prolong Gold (Life Technologies). Tumor sections were incubated with rat anti-mouse F4/80 followed by horseradish peroxidase (HRP)-labeled goat anti-rat IgG (DAKO) and tyramide green (Invitrogen). Sections were microwaved in 0.01M sodium citrate (pH 6) for 5 mins, re-blocked and probed with rabbit anti galectin-3 (R&D) or rabbit anti Ym1 followed by HRP-labeled goat anti-rabbit IgG (DAKO) and tyramide red (Invitrogen) and mounted in fluoromount-G with DAPI (eBioscience). Images were captured on a Nikon Eclipse E600 microscope.

RNA Extraction and RT-PCR

Total RNA from LLC1 tumors and lung tissue was prepared using RNeasy kits (Qiagen) and reverse transcribed into cDNA using Quantitect RT kits (Qiagen). cDNA was analyzed using either a SYBR green-based quantitative fluorescence method (Invitrogen) and Kiqstart primers (Sigma Aldrich) or Taqman primer probe sets (Life Technologies).

SDS PAGE and Western Blotting

Cells were lysed in NP-40 (Invitrogen) and separated by 10-15% SDS-PAGE. Proteins were transferred to nitrocellulose membrane and probed using antibodies against galectin-3, 1:500 (eBioM3/38, eBioscience) and GAPDH, 1:3000 (14C10, Cell Signaling Technology) followed by species specific HRP-conjugated secondary antibodies (Dako). Bound antibodies were detected using the enhanced chemiluminescence 2 detection kit (Pierce).

Tumor Dissociation and Flow cytometry

Tumors were minced in serum-free DMEM and digested with Liberase (2mg/ml; Sigma-Aldrich) and DNase I (Sigma-Aldrich) at 37°C for 30mins. Disaggregated tissue was filtered through a 35µm nylon mesh, washed and resuspended in FACS buffer (PBS with 0.1% bovine serum albumin (BSA)). Fc receptors were blocked with anti-mouse CD16/32 (Biolegend). Antibody cocktails (anti-mouse Ly6G-pacific blue, CD11b-BV605, Galectin-3-FITC, CD45-PerCP and CD45-APCcy7, MHC-II-PE, CD206-PEcy7, PD1-APC, F480-AF700, CD4-pacific blue, PD-L1 BV605, CD3-PerCPcy5.5, IFN γ -PE, CD8-AF700, all from Biolegend) were added to cells and incubated for 20mins at room temperature. Samples were fixed and RBCs were

simultaneously lysed in RBC Lysis/Fixation solution (Biolegend). For intracellular staining, cells were permeabilized with intracellular staining permeabilisation wash buffer (Biolegend) and incubated with anti-CD206 or anti-IFN γ (Biolegend). Cells were analyzed using an LSR-Fortessa cell analyser (Beckton Dickinson).

Statistics

Statistical analyses were performed using Graphpad Prism 7.0 software. Results are represented as mean \pm S.E.M and statistical tests are described in the figure legends.

Results

Galectin-3^{-/-} mice do not support the growth and metastasis of LLC1 tumors

To examine lung cancer growth within the correct tissue compartment LLC1 cells stably expressing *G. princeps*-luciferase were injected (1×10^3 cells) through the intercostal space directly into the lung parenchyma of control and galectin-3^{-/-} mice. H&E staining of lung tissue confirmed the presence of tumors in control but not galectin-3^{-/-} mouse lungs (**Figure 1A**). At 20 days post-injection 4/10 of control mice had tumors, while none of the galectin-3^{-/-} mice developed tumors (**Table 1**). In addition, 7/10 control animals displayed gross swelling of the mediastinal lymph nodes (MLN) (**Table 1**), which were positive for metastatic cells as assessed by luciferase assay on homogenized MLNs. Only 1/11 of galectin-3^{-/-} mice had luciferase positive MLNs (**Table 1**).

LLC1 cells expressing luciferase were injected subcutaneously (s.c) in both flanks of WT and galectin-3^{-/-} mice (n=12). After day 10, s.c. tumors from control animals were much larger than those of galectin-3^{-/-} mice. This difference became statistically significant at day 12 ($p=0.0004$). By the end of the study, tumors of controls had an average volume of 286mm^3 compared to a volume of 9mm^3 in galectin-3^{-/-} animals (96.9% reduction, $p<0.0001$) (**Figure 1B, C**). The weight of tumors from control mice was 98% heavier than that of galectin-3^{-/-} mice, $153 \pm 31\text{mg}$ and $3 \pm 2\text{mg}$ respectively ($p<0.0001$) (**Figure 1D**). Of all the tumor cell injections received by each group, only 11/40 led to tumors in galectin-3^{-/-} mice compared to 36/40 in controls (**Table 1**). 5/12 control mice had luciferase positive metastases

in their mediastinal lymph nodes (MLN) while galectin-3^{-/-} mice had no metastases (**Table 1**). These results indicate that galectin-3^{-/-} mice do not support tumor establishment and spread in a s.c. LLC1 model. Although LLC1 inoculation increased the serum concentrations of anti-galectin-3 IgG antibodies in galectin-3^{-/-} mice, no correlation, either negative or positive, was established between antibody production and tumor volume (**Figure S1**).

M2 macrophages are reduced in tumors from galectin-3^{-/-} mice

Tumor stroma F4/80⁺ macrophages were significantly higher in galectin-3^{-/-} animals compared to control (p=0.0217). However, the ratio of Ym1⁺/F480⁺ macrophages was significantly higher in controls (p=0.0484, **Figure 2A, B**), indicating that higher galectin-3 levels around the tumor environment can drive expansion of M2 macrophages (28). Transcript analysis from whole tumor RNA showed that control tumors had 2.5-, 3.3- and 16.7-fold higher levels of IL-4, IL-10 and IL-13 transcripts respectively (p=0.04, 0.024, 0.119 respectively), and displayed a 28.8-fold reduction in IFN- γ mRNA when compared to galectin-3^{-/-} tumors (p=0.0066, **Figure 2C**). These results indicate a cytokine environment that favors M2 macrophage activation in tumors of control but not galectin-3^{-/-} hosts and suggests an important role for galectin-3 in the regulation of TAM phenotype.

Macrophage depletion impairs tumor initiation

We hypothesized that tumor macrophages may contribute to tumor growth in the LLC1 model. C57Bl/6 CD11b-DTR transgenic mice were used as a model of macrophage ablation (33). CD11b-DTR transgenic mice and WT siblings received a single diphtheria toxin (DT) injection immediately prior to cell implant. At day 12, 15/24 tumors developed in CD11b-

DTR mice compared to 20/22 in controls. CD11b-DTR animals had significantly smaller tumor volumes compared to controls ($29.4 \pm 4.1 \text{ mm}^3$ and $89.4 \pm 0.9 \text{ mm}^3$ respectively) ($p=0.0005$) (**Figure 2D**) and significantly reduced tumor weights ($9.1 \pm 1.0 \text{ mg}$ and $23.4 \pm 4.0 \text{ mg}$ respectively) ($p=0.0011$) (**Figure 2E**). To assess the efficiency of macrophage ablation in this model DT was administered to mice with established tumors and F4/80 staining carried out 24h after DT administration. An 88% reduction in TAMs was observed in the tumors of DTR transgenic animals ($p<0.0001$) (**Figure S2A**). LLC1 cells *in vitro* display cell surface and cytoplasmic galectin-3 staining and release galectin-3 into the culture medium (**Figure S3A**). To determine whether tumor-derived galectin-3 contributes to tumor growth galectin-3 was stably knocked down (KD) in LLC1 cells prior to s.c. injection (**Figure S3B**). Although LLC1 proliferation was reduced by galectin-3 KD *in vitro* (**Figure S3C,D**), tumor growth and final tumor weights of LLC1-galectin-3-KD cells was similar to WT cells (**Figure S3E-G**).

Galectin-3 phenotype of bone marrow derived cells in the tumor microenvironment determine LLC1 tumor growth

Tumor galectin-3 had no effect on tumor growth so we altered galectin-3 expression in recruited cells. Control and galectin-3^{-/-} mice were irradiated and transplanted with 10^7 control or galectin-3^{-/-} bone marrow (BM) cells. Eight weeks post-BM transplant, LLC1 cells were injected subcutaneously. Transplantation of control BM cells into galectin-3^{-/-} mice resulted in significantly increased average tumor volume and final tumor weight compared to mice transplanted with galectin-3^{-/-} BM cells (final tumor volume 336mm^3 and final weight of 297.6mg compared to 163.9mm^3 and 124.4mg $p<0.0001$ and $p=0.0007$ respectively **Figure 2F,G**). Dual immunofluorescence staining showed that the stroma of tumors harvested from

galectin-3^{-/-} animals transplanted with control BM had F4/80 and galectin-3 dual positive cells (**Figure 2H**) although the total number of infiltrating macrophages was not different between control or galectin-3^{-/-} BM transplanted mice (**Figure S2B**) suggesting that galectin-3 positive macrophages are recruited to the tumor stroma and contribute to tumor growth.

High affinity galectin-3 inhibitor prevents human lung adenocarcinoma growth *in vivo*

Recently a series of monosaccharide galectin-3 inhibitors with low nM affinities and good selectivity over other galectins have been described (32). From this series GB1107 has high affinity in man at 37 nM but due to species differences in the galectin-3 carbohydrate binding domain (CBD), the mouse galectin-3 affinity is 38 fold lower. GB1107 has low clearance (1.2 ml/min/kg, t_{1/2} 4.5 h, i.v.) and good uptake upon oral administration resulting in high oral availability (F = 75 %, p.o). As a consequence, dosing GB1107 at 10 mg/kg orally once daily results in a plasma concentration above mouse K_d over 24h (**Figure S4**). CD-1 nude mice bearing human lung A549 adenocarcinoma xenografts were treated from day 18-post implantation once daily with 10mg/kg GB1107. This resulted in significantly reduced tumor growth and final tumor weights (46.2% smaller compared to vehicle control tumors with final average weights of 117 ± 16mg and 63 ± 11mg respectively (p=0.0132), **Figure 3A**). Treatment with GB1107 also inhibited growth (tumor volumes decreased 48% compared to controls on day 18, p<0.001) and reduced final tumor weights (47 ± 14mg versus 120 ± 29mg controls, p=0.0524) when administered daily from the outset (**Figure 3B**). Transcript analysis of tumor RNA from the LLC tumors revealed reduced galectin-3 (48% less than vehicle, p=0.018) and mesenchymal markers TGF-β (45% less than vehicle, p=0.015) and trends for

reductions of VEGF and α -SMA expression (**Figure 3D and S8C**). There was also a trend towards a reduction in expression of the M2 marker Ym1 (50% less than vehicle) and CD98 (49% less than vehicle), which drives galectin-3 mediated M2 macrophage activation (28), suggesting a decrease in M2 skewed TAM accumulation in the tumor. To examine effects on metastasis, LLC1 cells were injected intravenously and lung colonization was determined at 7 days post injection (**Figure 3C**). The presence of metastasis was examined by expression of Gaussia luciferase transcript in whole lung RNA extracts. GB1107 significantly reduced tumor burden by 79.2%. These data suggest that inhibition of galectin-3 with an orally active selective galectin-3 inhibitor can significantly reduce lung adenocarcinoma growth and metastasis *in vivo*. Mice were generated which express the human LGALS3 gene in place of the mouse gene (Hu-Gal-3-KI). Western blot confirmed expression of only human galectin-3 in mouse liver lysates from Hu-Gal-3-KI mice (**Figure 3F**). LLC tumor growth was inhibited by GB1107 in Hu-Gal-3-KI mice when administration was delayed until day 5 after inoculation (**Figure 3E**).

Galectin-3 inhibitor blocks LLC-induced alternative macrophage activation

Given the altered M1:M2 TAM ratio in LLC tumors from galectin-3^{-/-} mice and inhibitor treated mice we next determined the role of LLC derived galectin-3 on macrophage polarization. Conditioned media from LLC1 cells *in vitro* increased IL-4-stimulated arginase activity in bone marrow-derived macrophages (BMDMs) and increased gene expression of arginase-1 and fizz1 (**Figure S5A, C**). This increase was inhibited by GB1107 suggesting galectin-3 secreted by LLC1 cells induces macrophages to adopt an alternative M2-like phenotype (**Figure S5A, C**). GB1107 did not affect LPS-induced Nos2 expression or nitric oxide (NO) production by

BMDMs (**Figure S5A, B**). Although our data show TAMs to be a vital determinant of tumor growth *in vivo*, treatment of LLC1 cells with inhibitor *in vitro* also impacted on cell proliferation and migration albeit at higher concentrations (**Figure S5D-F**), suggesting some direct effect on galectin-3 mediated-tumor cell expansion and migration.

Galectin-3 depletion reduces M2-like macrophages and enhances infiltration of activated CD8 T cells

TAMs can contribute to T cell immunosuppression (4). In particular, M2-like macrophages secrete more galectin-3 (34) and galectin-3 directly impedes T cell infiltration and activation (24-27, 35). We therefore investigated whether galectin-3 dependent M2 polarization is also associated with changes in T cell infiltration and activation *in vivo*. Flow cytometric analysis of tumor digests (see Figure S6 for gating strategy) from hu-Gal-3-KI mice treated with GB1107 showed no increase in macrophage infiltration, but showed a decrease in macrophage CD206 expression indicative of reduced M2 TAMs (**Figure 4A**). Similarly, while there was no significant change in the total number of CD3⁺ T cells, GB1107 caused an increase in CD8⁺ but not CD4⁺ T cells within tumors (**Figure 4A**). This pattern of immune infiltration was also observed in tumor digests from galectin-3^{-/-} mice compared to WT C57Bl/6 mice (**Figure 4B**). Moreover, in galectin-3^{-/-} tumors, infiltrating CD8 T cells but not CD4⁺ T cells displayed trends toward increased PD-1 and IFN- γ expression, together suggesting that galectin-3 depletion may reprogram the tumor microenvironment to favor pro-inflammatory M1-like macrophages and enhance cytotoxic CD8 T cell infiltration and activation. Galectin-3^{-/-} mouse tumors displayed no overall changes in total CD45⁺ cells, neutrophils, monocytes or dendritic cells (DCs) compared to WT tumors (**Figure S6**).

To assess whether other systemic changes in galectin-3 depleted mice may also influence CD8 T cell activation, we assessed myeloid populations within the bone marrow of WT and galectin-3^{-/-} mice. We observed no differences in total CD11b⁺ cells, neutrophils or monocytes including inflammatory Ly6C^{hi} monocytes (**Figure S7**). There were however increased DCs in galectin-3^{-/-} compared to WT mice, suggestive of another indirect mechanism by which galectin-3 may enhance anti-tumor T cell priming (26).

Galectin-3 inhibitor potentiates the anti-tumor effects of PD-L1 blockade

We next examined the effect of galectin-3 inhibition in combination with immune checkpoint inhibition. In this study GB1107 treatment was delayed until day 6 post implantation. Delayed administration of GB1107 alone did not reduce tumor burden and administration of an anti-PD-L1 antibody administered twice weekly I.P from day 6 also had no impact on tumor growth. However, a combination of GB1107 and anti-PD-L1 antibody treatment significantly potentiated the effect of the single agents (49.5% and 51.4% reduced tumor volumes and weights respectively compared with untreated controls, (**Figure 5A,B**) and there was corresponding reduction in galectin-3 protein levels within GB1107 treated tumors (**Figure S8F**).

The reduced tumor growth in the combination group was not associated with changes in tumor cell proliferation as determined by Ki-67 IHC staining (**Figure S8D, E**) but was instead associated with an increase in PD-1⁺ CD8⁺ T cells (**Figure 5C, S8A-B**) and reduced CD206 expression in macrophages (**Figure 5C**). This was combined with a significant increase in expression of T cell cytotoxic mediators (IFN- γ perforin-1, granzyme B and fas ligand; **Figure**

5D) and a 10.3% increase ($p=0.005$) in the apoptosis marker cleaved caspase-3 (**Figure 5F,G**).

Together our data suggests that combination therapy with galectin-3 inhibitor GB1107 and PD-L1 blocking antibody promotes tumor cell apoptosis and cytotoxic CD8 T cell activation.

Discussion

In this study we show that galectin-3^{-/-} mice do not support LLC1 tumor growth and deleting galectin-3 in bone marrow derived cells recruited to engrafted mouse lung adenocarcinomas inhibits tumor growth and spread despite high expression of galectin-3 in the tumor cells. Furthermore, macrophage depletion reduces monocyte recruitment and LLC1 tumor growth, confirming that depletion of macrophages with liposomal clodronate inhibits LLC1 tumor growth (36). Although the spleen can be an important source of TAMs in a KRAS and P53 driven model of lung adenocarcinoma (37), the bone marrow compartment has been shown to be the major source of TAMs in the LLC1 model (38). Therefore, we sought to restore galectin-3 in tumor macrophages in galectin-3^{-/-} mice by bone marrow transplant with wild type galectin-3 +ve bone marrow cells. This results in an increase in tumor growth similar to that observed in wild type mice. Our previous work has shown that galectin-3 is an important regulator of macrophage function, promoting an “M2” phenotype (28). Our data shows that macrophages in tumors from galectin-3^{-/-} mice or mice treated with GB1107 have reduced CD206⁺ M2-like macrophages and we observe reduced M2-promoting cytokine transcripts and elevated IFN- γ expression within galectin-3^{-/-} tumors. In addition, conditioned media from LLC cells increases alternative activation of macrophages *in vitro* and this can be blocked by co-culture with

GB1107. This demonstrates that galectin-3 contributes to the M2 immunosuppressive function of TAMs.

TAMs promote many important features of tumor progression including angiogenesis, tumor cell invasion, motility, and metastasis and can also suppress T cell responses (4). This data shows that galectin-3 expressing macrophages are recruited to the tumor site, develop an M2 phenotype and induce down regulation of CD8⁺ CTL functions. Galectin-3 has been shown to induce T cell tolerance resulting in T cell anergy, through various mechanisms including inhibiting CD8 and TCR clustering (39), destabilizing the immune synapse and promoting internalization of TCR and CD3 ζ chains (40). It can also restrict membrane movement and TCR-associated signaling functions of CD45 (41) and inhibit LFA-1 recruitment thus disrupting proper secretory synapse formation and secretion of IFN- γ (27).

Galectin-3 may also suppress CTL effector function by binding to LAG-3, a negative regulatory checkpoint, on CD8⁺ T cells (26) and by inducing apoptosis of CTLs (25) and impairs the anti-tumor functions of natural killer (NK) cells (42). CTLs activated *in vitro* show an alteration in the *N*-glycome with longer and more branched *N*-glycans resulting in the expression of surface glycoproteins that exhibit high galectin-3 binding (43). The high concentration of galectin-3 found in tumor microenvironments could potentially explain the loss of CTL functions through reduced motility and signaling functions of surface molecules.

Galectin-3^{-/-} mice have also been shown to have an increase in lymph node plasmacytoid DCs (pDCs) compared to WT mice which are superior in activating CD8⁺ CTLs compared to conventional DC (26). In addition, galectin-3 knockdown in monocyte derived DCs increases the proliferation and IFN- γ production from antigen-stimulated CD4⁺ T cells (44). Our profiling of

bone marrow from WT and gal-3 KO mice showed an increase in CD45⁺/MHC-II⁺/CD11b⁺ DCs in bone marrow of gal-3 KO mice compared to WT. Although our study did not distinguish DC subsets, together the data suggests that galectin-3 may indirectly regulate CD8 function by promoting pDC or other DC subset functions. This requires further study.

We show that treatment with GB1107 alone from the outset inhibits LLC1 growth and delayed treatment inhibits LLC1 growth in human galectin-3 expressing mice. This reflects the increased affinity this inhibitor has on human versus mouse galectin-3. In addition, the galectin-3 inhibitor significantly potentiates the effect of immune checkpoint blockade with an anti-PD-L1 blocking antibody. It is believed that the limited patient responses to checkpoint inhibition is attributable to the lack of T-cell infiltration in so-called ‘cold’ tumors (2). Gordon-Alonso *et al.*, show that galectin-3 binds to the extracellular matrix and to glycosylated IFN- γ , preventing release of IFN- γ -induced CXCL9 which acts as a T cell chemo-attractant (35). Consistent with this, GB1107 both alone or in combination with anti-PD-L1 increases the number of tumor infiltrating CD8 CTLs. Therefore galectin-3 inhibition might provide the critical means to turn a ‘cold’ tumor ‘hot’, and thus responsive to immune checkpoint intervention. Furthermore CD8⁺ CTLs within the combination drug-treated tumors are more activated (express more surface PD-1), and the cytokine environment favors tumor rejection with increased expression of cytotoxic (IFN- γ , perforin-1 and granzyme B) and apoptotic (fas ligand) genes with increased caspase activation.

Reduced galectin-3 expression within tumor cells has been shown to reduce tumor growth in many cancers (reviewed in (45)), suggested to be due to the anti-apoptotic effect of cytoplasmic galectin-3 binding to K-RAS and engaging anti-apoptotic pathways via its NWGR motif (20). However, we show that knockdown of galectin-3 in tumor cells with shRNA had only a partial effect on tumor growth *in vitro* but had no significant effect on LLC1 growth *in vivo*. We also

show that treatment with the galectin-3 inhibitor alone could inhibit human adenocarcinoma growth in CD-1 nude mice, which lack a T cell response but which display innate immunity. This suggests that either tumor derived or macrophage derived galectin-3 can impact on tumor growth in this model, independent of the T-cell mediated effects.

In conclusion, our results demonstrate that galectin-3 inhibition leads to a reduction in M2-like TAMs and increased infiltration and activity of CD8⁺ CTLs within LLC1 tumors resulting in reduced tumor growth and metastasis. Several studies have used other approaches to inhibit galectin-3 in cancer including peptide inhibitors (46), lactulose amines (47), a glycopeptide isolated from cod (48) and large complex plant-derived polysaccharides including modified citrus pectin (49), GCS-100 (39) and galactomannans such as GM-CT-01 (50). GCS-100 is currently being developed for chronic lymphoid leukemia and multiple myeloma (51). However recent evidence suggests that these complex carbohydrates do not act as inhibitors of the canonical carbohydrate-binding site of galectin-3 and their physiological effects may be due to unrelated actions (52). We show using a specific and high affinity inhibitor of the galectin-3 carbohydrate site that pharmacological inhibition of galectin-3 inhibits lung adenocarcinoma growth and potentiates the effect of immune checkpoint inhibitors. Therefore galectin-3 has a strong regulatory effect on cancer related inflammation and could present a key target in the management of lung, and potentially other galectin-3 driven carcinomas, in combination with immune checkpoint blockade.

Acknowledgments:

We thank Frank McCaughan for helpful discussions and kind provision of reagents, as well as

the Biomedical Research Council Flow Cytometry Core (King's College) and the University of Edinburgh Queen's Medical Research Institute's Flow Cytometry facility for flow sorting and flow cytometric analysis.

Author contributions:

L.V., E.K., A.C.M. conceived and performed experiments and wrote the manuscript, A.C.M., H.S. and T.S. conceived experiments and secured funding, C.R. and B.M. performed experiments, F.Z., U.J.N., H.L., P.F., A.P, L.G., S.T. and H.S. provided reagents and expertise. S.E.M.H., C.G., S.J.F., N.C.H. and M.K.B.W. provided expertise and feedback.

References:

1. Quaresma M, Coleman MP, Rachet B. 40-year trends in an index of survival for all cancers combined and survival adjusted for age and sex for each cancer in England and Wales, 1971-2011: a population-based study. *Lancet*. 2015;385(9974):1206-18.
2. Sharma P, Hu-Lieskovan S, Wargo JA, Ribas A. Primary, Adaptive, and Acquired Resistance to Cancer Immunotherapy. *Cell*. 2017;168(4):707-23.
3. Yuan A, Hsiao YJ, Chen HY, Chen HW, Ho CC, Chen YY, et al. Opposite Effects of M1 and M2 Macrophage Subtypes on Lung Cancer Progression. *Scientific reports*. 2015;5:14273.
4. Noy R, Pollard JW. Tumor-associated macrophages: from mechanisms to therapy. *Immunity*. 2014;41(1):49-61.
5. Gordon SR, Maute RL, Dulken BW, Hutter G, George BM, McCracken MN, et al. PD-1 expression by tumour-associated macrophages inhibits phagocytosis and tumour immunity. *Nature*. 2017;545(7655):495-9.
6. Arlauckas SP, Garriss CS, Kohler RH, Kitaoka M, Cuccarese MF, Yang KS, et al. In vivo imaging reveals a tumor-associated macrophage-mediated resistance pathway in anti-PD-1 therapy. *Science translational medicine*. 2017;9(389).
7. Neubert NJ, Schmittnaegel M, Bordry N, Nassiri S, Wald N, Martignier C, et al. T cell-induced CSF1 promotes melanoma resistance to PD1 blockade. *Science translational medicine*. 2018;10(436).
8. Peranzoni E, Lemoine J, Vimeux L, Feuillet V, Barrin S, Kantari-Mimoun C, et al. Macrophages impede CD8 T cells from reaching tumor cells and limit the efficacy of anti-PD-1 treatment. *Proceedings of the National Academy of Sciences of the United States of America*. 2018;115(17):E4041-E50.
9. Hirabayashi J, Hashidate T, Arata Y, Nishi N, Nakamura T, Hirashima M, et al. Oligosaccharide specificity of galectins: a search by frontal affinity chromatography. *Biochim Biophys Acta*. 2002;1572(2-3):232-54.
10. Chen HY, Liu FT, Yang RY. Roles of galectin-3 in immune responses. *Arch Immunol Ther Exp (Warsz)*. 2005;53(6):497-504.
11. Liu FT, Hsu DK, Zuberi RI, Kuwabara I, Chi EY, Henderson WR, Jr. Expression and function of galectin-3, a beta-galactoside-binding lectin, in human monocytes and macrophages. *The American journal of pathology*. 1995;147(4):1016-28.
12. Joo HG, Goedegebuure PS, Sadanaga N, Nagoshi M, von Bernstorff W, Eberlein TJ. Expression and function of galectin-3, a beta-galactoside-binding protein in activated T lymphocytes. *Journal of leukocyte biology*. 2001;69(4):555-64.
13. Dube-Delarosbil C, St-Pierre Y. The emerging role of galectins in high-fatality cancers. *Cellular and molecular life sciences : CMLS*. 2018;75(7):1215-26.
14. Mathieu A, Saal I, Vuckovic A, Ransy V, Vereerstraten P, Kaltner H, et al. Nuclear galectin-3 expression is an independent predictive factor of recurrence for adenocarcinoma and squamous cell carcinoma of the lung. *Modern pathology : an official journal of the United States and Canadian Academy of Pathology, Inc*. 2005;18(9):1264-71.
15. Puglisi F, Minisini AM, Barbone F, Intersimone D, Aprile G, Puppini C, et al. Galectin-3 expression in non-small cell lung carcinoma. *Cancer letters*. 2004;212(2):233-9.
16. Yu LG. Circulating galectin-3 in the bloodstream: An emerging promoter of cancer metastasis. *World journal of gastrointestinal oncology*. 2010;2(4):177-80.
17. Reticker-Flynn NE, Malta DF, Winslow MM, Lamar JM, Xu MJ, Underhill GH, et al. A combinatorial extracellular matrix platform identifies cell-extracellular matrix interactions that correlate with metastasis. *Nature communications*. 2012;3:1122.
18. Wu F, Hu N, Li Y, Bian B, Xu G, Zheng Y. Galectin-3 genetic variants are associated with platinum-based chemotherapy response and prognosis in patients with NSCLC. *Cellular oncology*. 2012;35(3):175-80.
19. Honjo Y, Nangia-Makker P, Inohara H, Raz A. Down-regulation of galectin-3 suppresses tumorigenicity of human breast carcinoma cells. *Clinical cancer research : an official journal of the American Association for Cancer Research*. 2001;7(3):661-8.
20. Akahani S, Nangia-Makker P, Inohara H, Kim HR, Raz A. Galectin-3: a novel antiapoptotic molecule with a functional BH1 (NWGR) domain of Bcl-2 family. *Cancer research*. 1997;57(23):5272-6.

21. Radosavljevic G, Jovanovic I, Majstorovic I, Mitrovic M, Lisnic VJ, Arsenijevic N, et al. Deletion of galectin-3 in the host attenuates metastasis of murine melanoma by modulating tumor adhesion and NK cell activity. *Clin Exp Metastasis*. 2011;28(5):451-62.
22. Chung LY, Tang SJ, Wu YC, Sun GH, Liu HY, Sun KH. Galectin-3 augments tumor initiating property and tumorigenicity of lung cancer through interaction with beta-catenin. *Oncotarget*. 2015;6(7):4936-52.
23. Markowska AI, Jefferies KC, Panjwani N. Galectin-3 protein modulates cell surface expression and activation of vascular endothelial growth factor receptor 2 in human endothelial cells. *The Journal of biological chemistry*. 2011;286(34):29913-21.
24. Ruvolo PP. Galectin 3 as a guardian of the tumor microenvironment. *Biochim Biophys Acta*. 2016;1863(3):427-37.
25. Peng W, Wang HY, Miyahara Y, Peng G, Wang RF. Tumor-associated galectin-3 modulates the function of tumor-reactive T cells. *Cancer Res*. 2008;68(17):7228-36.
26. Kouo T, Huang L, Pucsek AB, Cao M, Solt S, Armstrong T, et al. Galectin-3 Shapes Antitumor Immune Responses by Suppressing CD8+ T Cells via LAG-3 and Inhibiting Expansion of Plasmacytoid Dendritic Cells. *Cancer immunology research*. 2015;3(4):412-23.
27. Petit AE, Demotte N, Scheid B, Wildmann C, Bigirimana R, Gordon-Alonso M, et al. A major secretory defect of tumour-infiltrating T lymphocytes due to galectin impairing LFA-1-mediated synapse completion. *Nature communications*. 2016;7:12242.
28. MacKinnon AC, Farnworth SL, Hodgkinson PS, Henderson NC, Atkinson KM, Leffler H, et al. Regulation of alternative macrophage activation by galectin-3. *Journal of immunology*. 2008;180(4):2650-8.
29. Voss JJ, Ford CA, Petrova S, Melville L, Paterson M, Pound JD, et al. Modulation of macrophage antitumor potential by apoptotic lymphoma cells. *Cell Death Differ*. 2017.
30. Hsu DK, Yang RY, Pan Z, Yu L, Salomon DR, Fung-Leung WP, et al. Targeted disruption of the galectin-3 gene results in attenuated peritoneal inflammatory responses. *The American journal of pathology*. 2000;156(3):1073-83.
31. Cailhier JF, Partolina M, Vuthoori S, Wu S, Ko K, Watson S, et al. Conditional macrophage ablation demonstrates that resident macrophages initiate acute peritoneal inflammation. *J Immunol*. 2005;174(4):2336-42.
32. Zetterberg FR, Peterson K, Johnsson RE, Brimert T, Hakansson M, Logan DT, et al. Monosaccharide Derivatives with Low-Nanomolar Lectin Affinity and High Selectivity Based on Combined Fluorine-Amide, Phenyl-Arginine, Sulfur-pi, and Halogen Bond Interactions. *ChemMedChem*. 2018;13(2):133-7.
33. Duffield JS, Forbes SJ, Constandinou CM, Clay S, Partolina M, Vuthoori S, et al. Selective depletion of macrophages reveals distinct, opposing roles during liver injury and repair. *J Clin Invest*. 2005;115(1):56-65.
34. Novak R, Dabelic S, Dumic J. Galectin-1 and galectin-3 expression profiles in classically and alternatively activated human macrophages. *Biochimica et biophysica acta*. 2012;1820(9):1383-90.
35. Gordon-Alonso M, Hirsch T, Wildmann C, van der Bruggen P. Galectin-3 captures interferon-gamma in the tumor matrix reducing chemokine gradient production and T-cell tumor infiltration. *Nature communications*. 2017;8(1):793.
36. Schmall A, Al-Tamari HM, Herold S, Kampschulte M, Weigert A, Wietelmann A, et al. Macrophage and cancer cell cross-talk via CCR2 and CX3CR1 is a fundamental mechanism driving lung cancer. *Am J Respir Crit Care Med*. 2015;191(4):437-47.
37. Cortez-Retamozo V, Etzrodt M, Newton A, Rauch PJ, Chudnovskiy A, Berger C, et al. Origins of tumor-associated macrophages and neutrophils. *Proceedings of the National Academy of Sciences of the United States of America*. 2012;109(7):2491-6.
38. Shand FH, Ueha S, Otsuji M, Koid SS, Shichino S, Tsukui T, et al. Tracking of intertissue migration reveals the origins of tumor-infiltrating monocytes. *Proceedings of the National Academy of Sciences of the United States of America*. 2014;111(21):7771-6.
39. Demotte N, Wieers G, Van Der Smissen P, Moser M, Schmidt C, Thielemans K, et al. A galectin-3 ligand corrects the impaired function of human CD4 and CD8 tumor-infiltrating lymphocytes and favors tumor rejection in mice. *Cancer Res*. 2010;70(19):7476-88.
40. Chen HY, Fermin A, Vardhana S, Weng IC, Lo KF, Chang EY, et al. Galectin-3 negatively regulates TCR-mediated CD4+ T-cell activation at the immunological synapse. *Proceedings of the National Academy of Sciences of the United States of America*. 2009;106(34):14496-501.
41. Stillman BN, Hsu DK, Pang M, Brewer CF, Johnson P, Liu FT, et al. Galectin-3 and galectin-1 bind distinct cell surface glycoprotein receptors to induce T cell death. *Journal of immunology*. 2006;176(2):778-89.
42. Rabinovich GA, Toscano MA. Turning 'sweet' on immunity: galectin-glycan interactions in immune tolerance and inflammation. *Nature reviews Immunology*. 2009;9(5):338-52.

43. Antonopoulos A, Demotte N, Stroobant V, Haslam SM, van der Bruggen P, Dell A. Loss of effector function of human cytolytic T lymphocytes is accompanied by major alterations in N- and O-glycosylation. *J Biol Chem.* 2012;287(14):11240-51.
44. Mobergslien A, Sioud M. Galectin-1 and -3 gene silencing in immature and mature dendritic cells enhances T cell activation and interferon-gamma production. *Journal of leukocyte biology.* 2012;91(3):461-7.
45. Wang L, Guo XL. Molecular regulation of galectin-3 expression and therapeutic implication in cancer progression. *Biomed Pharmacother.* 2016;78:165-71.
46. Zou J, Glinsky VV, Landon LA, Matthews L, Deutscher SL. Peptides specific to the galectin-3 carbohydrate recognition domain inhibit metastasis-associated cancer cell adhesion. *Carcinogenesis.* 2005;26(2):309-18.
47. Glinsky VV, Kiriakova G, Glinskii OV, Mossine VV, Mawhinney TP, Turk JR, et al. Synthetic galectin-3 inhibitor increases metastatic cancer cell sensitivity to taxol-induced apoptosis in vitro and in vivo. *Neoplasia.* 2009;11(9):901-9.
48. Guha P, Kaptan E, Bandyopadhyaya G, Kaczanowska S, Davila E, Thompson K, et al. Cod glycopeptide with picomolar affinity to galectin-3 suppresses T-cell apoptosis and prostate cancer metastasis. *Proceedings of the National Academy of Sciences of the United States of America.* 2013;110(13):5052-7.
49. Pienta KJ, Naik H, Akhtar A, Yamazaki K, Replogle TS, Lehr J, et al. Inhibition of spontaneous metastasis in a rat prostate cancer model by oral administration of modified citrus pectin. *J Natl Cancer Inst.* 1995;87(5):348-53.
50. Demotte N, Bigirimana R, Wieers G, Stroobant V, Squifflet JL, Carrasco J, et al. A short treatment with galactomannan GM-CT-01 corrects the functions of freshly isolated human tumor-infiltrating lymphocytes. *Clin Cancer Res.* 2014;20(7):1823-33.
51. Harazono Y, Nakajima K, Raz A. Why anti-Bcl-2 clinical trials fail: a solution. *Cancer Metastasis Rev.* 2014;33(1):285-94.
52. Stegmayr J, Lepur A, Kahl-Knutson B, Aguilar-Moncayo M, Klyosov AA, Field RA, et al. Low or no inhibitory potency of the canonical galectin carbohydrate binding site by pectins and galactomannans. *J Biol Chem.* 2016.

Orthotopic Tumors		
Genotype	No. of mice with primary tumors	No. of mice with LN metastases
WT	4/10 (40%)	7/10 (70%)
Gal-3 ^{-/-}	0/11 (0%)	1/11 (9%)
Subcutaneous Tumors		
Genotype	No. of mice with primary tumors	No. of mice with LN metastases
WT	36/40 (90%)	5/12 (41.7%)
Gal-3 ^{-/-}	11/40 (27.5%)	0/12 (0%)

Table 1. Galectin-3^{-/-} mice do not support tumor growth

Prevalence of mice with established primary tumors and inguinal lymph node metastases are summarized. Orthotopic and subcutaneous tumor data is representative of one or two independent experiments respectively.

Figure legends

Figure 1. Galectin-3^{-/-} mice do not support tumor growth

LLC1 cells were injected into the lung parenchyma of age and sex-matched C57Bl/6 wild type and galectin-3^{-/-} mice. Tumor nodules were enumerated by macroscopic counting and draining lymph nodes were checked for metastases by luciferase assay. Representative H&E-stained lung sections (A) from WT and galectin-3^{-/-} mice are shown. (B-D) LLC1 cells were inoculated subcutaneously into both flanks of WT or galectin-3^{-/-} mice. Representative images (B), tumor volume (C) and tumor weight on day 19 post-dissection (D) are shown. Arrows indicate tumor sites. Data in (A) is derived from a single experiment, n=10-11. Data from (B-D) are representative of two independent experiments, n=8; Differences were compared using an unpaired two-tailed t test; ***P<0.001, ****P<0.0001 (compared to WT on the same day).

Figure 2

Bone-marrow derived macrophages support LLC1 tumor growth.

(A) Subcutaneous tumors from WT or galectin-3^{-/-} mice were stained for F4/80 or Ym-1. (B) Quantitation of Ym1 and F480 staining in tumor sections. (C) RNA was extracted from these tumors and gene expression of various cytokines was assessed by qPCR. (D) LLC1 cells were injected subcutaneously in both flanks of CD11b DTR mice (n=12) and their wild type siblings (n=11). All mice were administered DT (10 ng/g) prior to cell injection. (E) Tumor volume and (F) tumor weights following DT administration. (G) WT and galectin-3^{-/-} mice were treated with clodronate, irradiated and subsequently transplanted with bone marrow cells from WT or galectin-3^{-/-} mice. LLC1 cells were injected subcutaneously into both flanks of transplanted mice

and tumor volumes (F) and weights (G) were measured. (H) Double IF staining for F4/80 (green) and galectin-3 (red) was performed in tumors from galectin-3^{-/-} mice receiving either WT or galectin-3^{-/-} bone marrow transplants. Dotted line represents the boundary between tumor cells (T) and stroma (S). Data is representative of 8 mice per irradiation/transplant control group and 12 mice per experimental group. Two-tailed t-tests were used to assess statistical differences; *P<0.05, ***P<0.001.

Figure 3

Galectin-3 inhibitor GB1107 inhibits lung adenocarcinoma growth and metastasis *in vivo*.

(A) Female CD-1 nude mice received two subcutaneous injections of 3x10⁶ A549 cells in a 1:1 ratio of matrigel and serum-free media. Tumors grew to an average of 166mm³ before commencement of single daily dosing of vehicle (n=6) or 10mg/kg GB1107 (n=6) from day 18. (A) Tumor volumes and weights, along with representative images are shown. (B) C57Bl/6 mice were injected subcutaneously with LLC1 cells and orally dosed once daily with vehicle or 10mg/kg GB1107 from day 1. Tumor volumes and weights are shown. (C) To test the effect of GB1107 on metastasis, mice were injected with 1x10⁶ LLC1 cells via the tail vein, followed by daily oral gavage of vehicle (n=10) or GB1107 (10mg/kg; n=10) from day 1. On day 7, tumor burden in whole lungs was determined by qPCR using luciferase-specific primers. (D) RNA was extracted from tumors from (B) and expression of various genes was evaluated by qPCR. (E) Hu-Gal-3-KI mice bearing bilateral subcutaneous LLC1 tumors received vehicle or 10 mg/kg GB1107 once daily orally from day 5. Tumor volumes and weights on day 14 are shown. Results from (E) represent the mean +/- SEM of 2 independent experiments of n=6. (F) Western blot

confirming expression of human galectin-3 in liver lysates from hu-Gal-3-KI mice. Two-tailed t-tests were used to determine statistical significance; * $P < 0.05$, ** $P < 0.01$, *** $P < 0.001$ (compared to vehicle controls).

Figure 4. Galectin-3 depletion reduces intra-tumor M2-like macrophages and CD8 T cell activation.

LLC tumors from human Hu-Gal-3-KI mice from Figure 3E treated with vehicle or GB1107 (n=6) were digested and processed by flow cytometry. (A) Relative prevalence of total macrophages and CD206 expression in macrophages and CD3+, CD4+ and CD8+ T cells in tumor digests. (B) Flow cytometry analysis of subcutaneous tumors from WT or galectin-3^{-/-} mice (n=4).

Figure 5

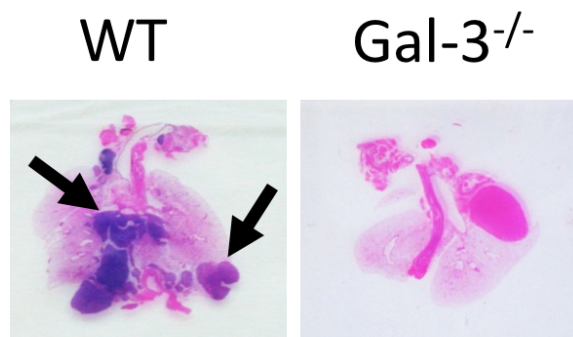
Combination therapy with galectin-3 inhibitor GB1107 and PD-L1 blocking antibody promote tumor cell apoptosis and cytotoxic CD8 T cell activation.

On day 6 mice bearing subcutaneous LLC1 tumors were randomized into 4 groups and received either no treatment (n=8), α -PD-L1 neutralizing antibody (200 μ g twice weekly I.P, n=8) or GB1107 (10mg/kg once daily orally, n=8) or α -PD-L1 plus GB1107 (n=8). Tumor volumes (A) and weights on day 16 (B) are shown. (C) Tumor infiltrating immune populations were analyzed by flow cytometry (n=4). (D) Total RNA was extracted from tumors in each group and qPCR was used to assess relative gene expression. (E-F) Immunohistochemical staining of cleaved caspase-3 was quantified as described in materials and methods. Scale bars are 100 μ m. Data

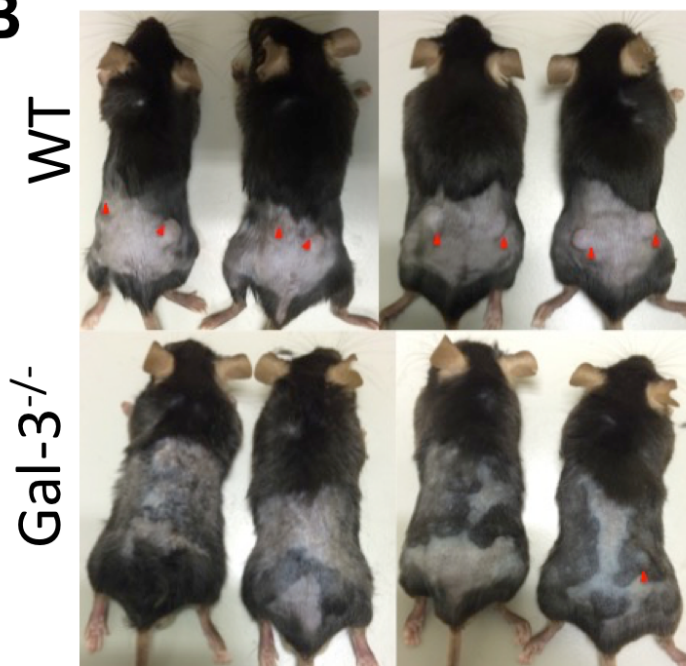
represents mean \pm SE from a single (A-B, D-F) or 2 (C) independent experiments. Two-way ANOVA with Tukey's Post Hoc test was used to test for differences in tumor volume and cleaved caspase-3 IHC scores. One-way ANOVA and Fisher's LSD test were used to compare tumor weights, and qPCR and flow cytometry data was compared using two-tailed t-tests; *P<0.05, **P<0.01, ***P<0.001.

Figure 1

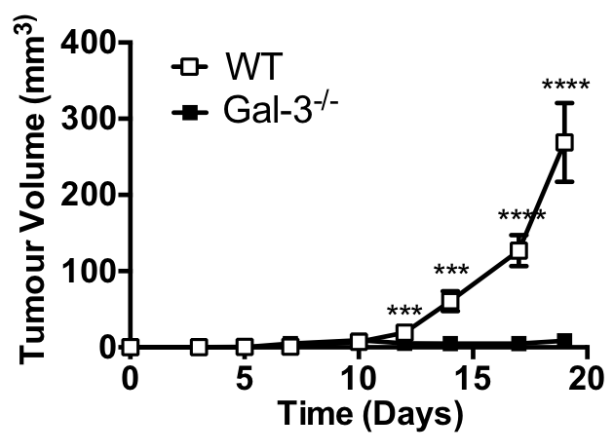
A Orthotopic tumors



B



C Subcutaneous tumors



D

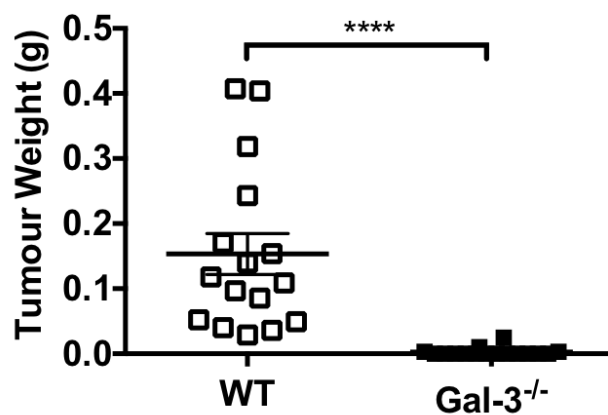
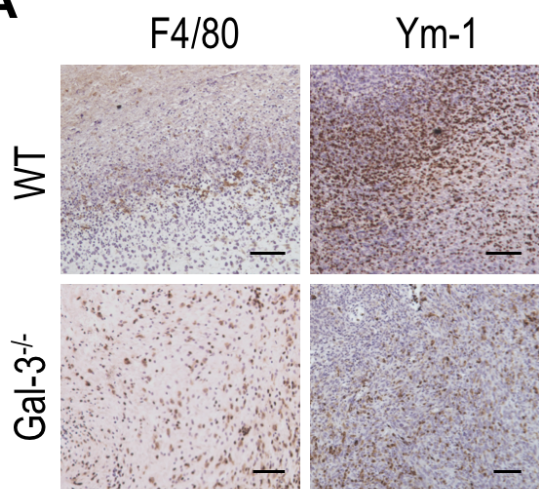
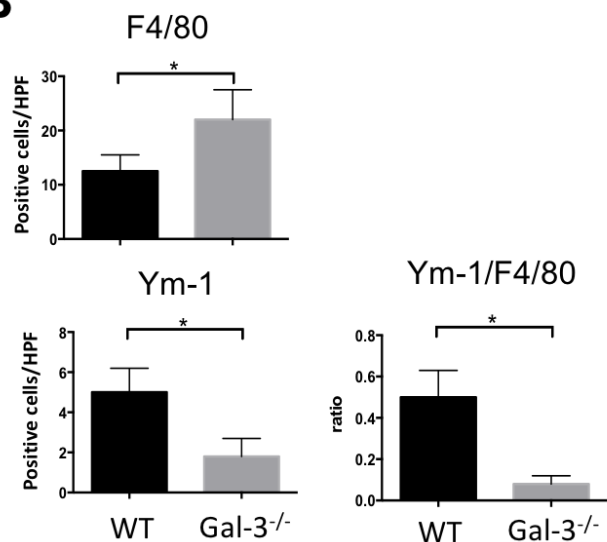


Figure 2

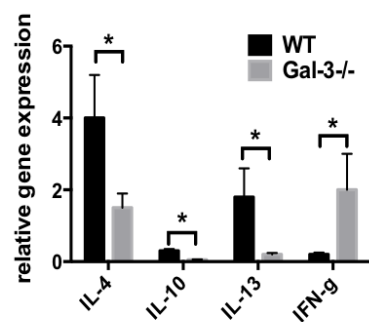
A



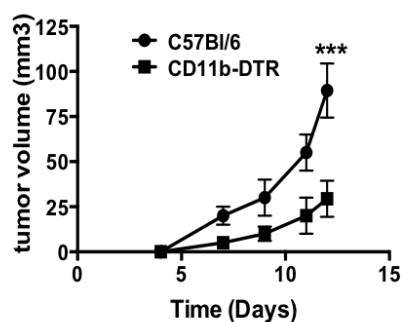
B



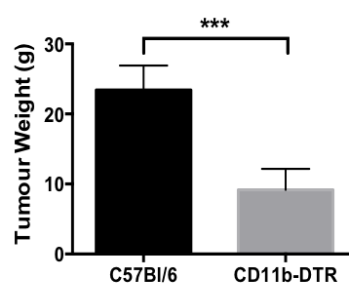
C



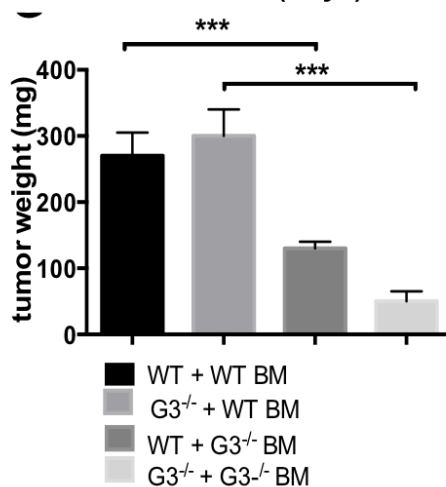
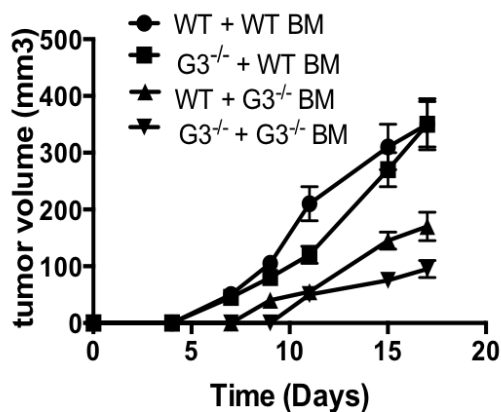
D



E



F



H

LLC1 tumors in gal-3^{-/-} mice

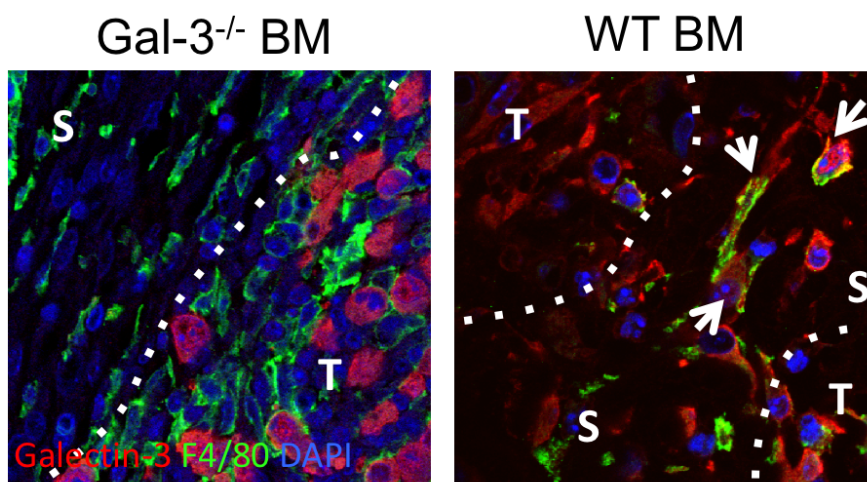
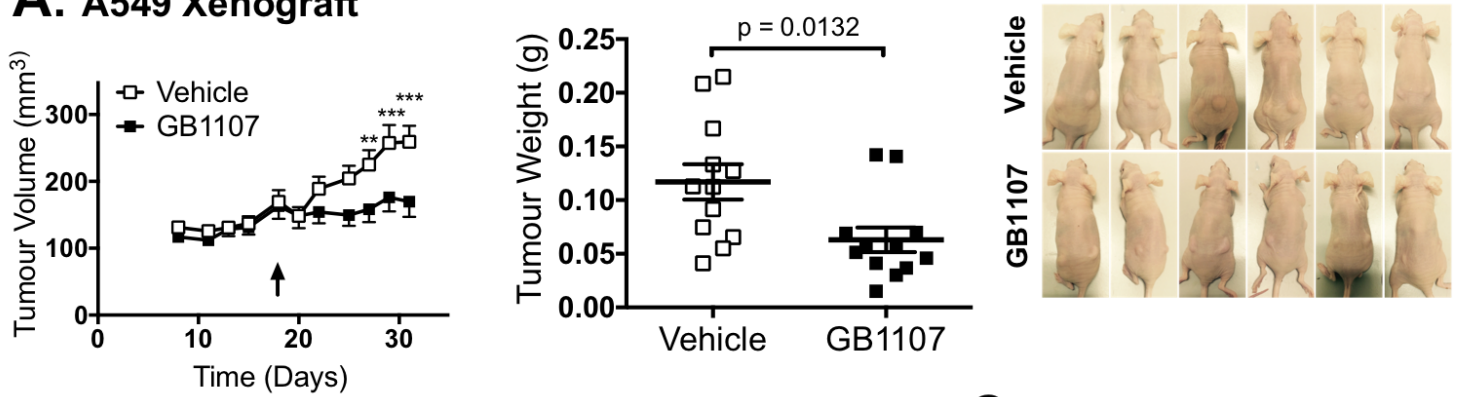
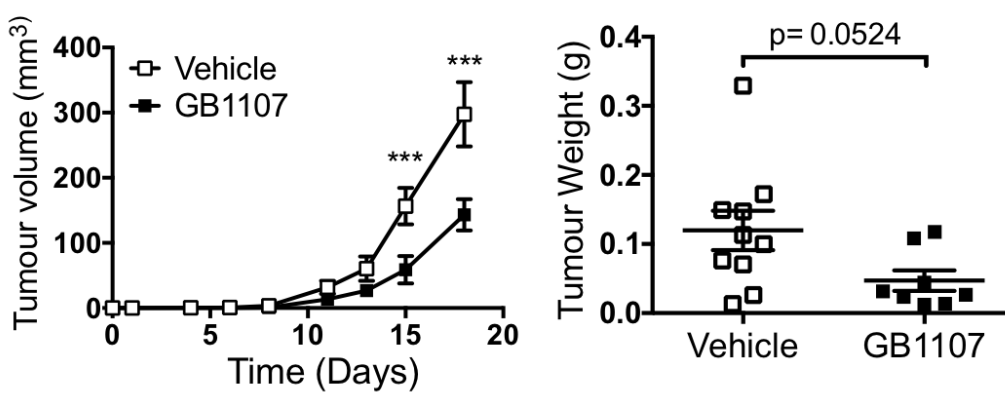


Figure 3

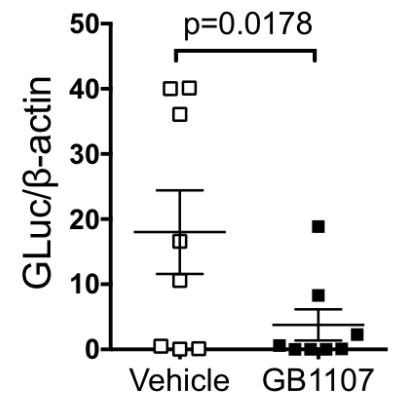
A: A549 Xenograft



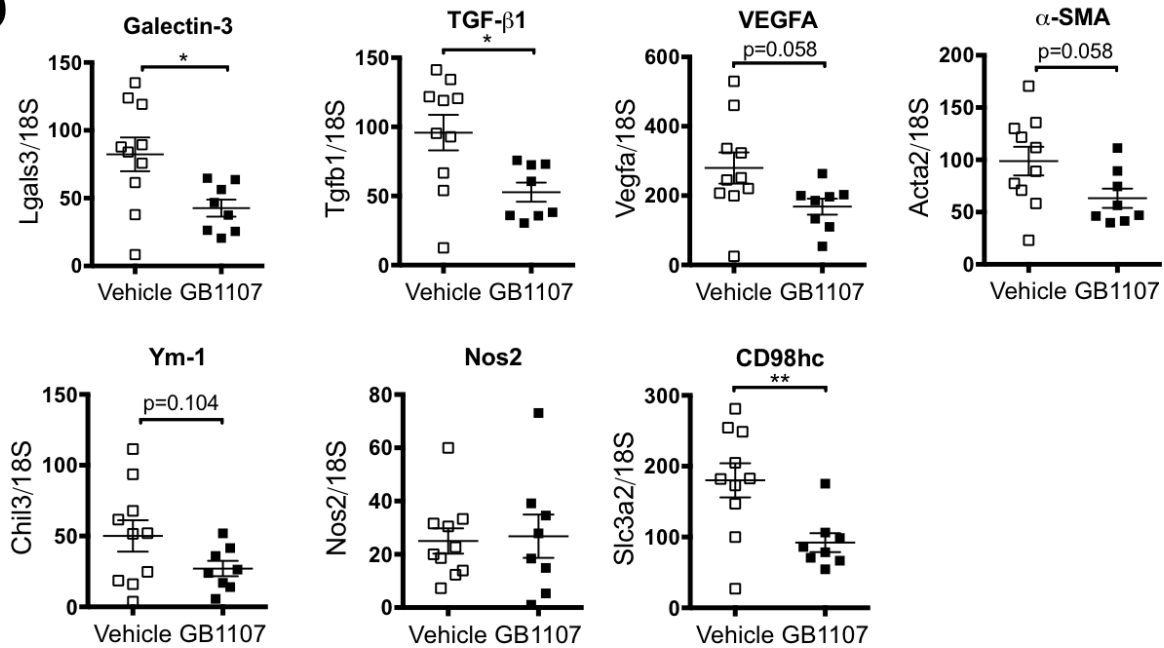
B: LLC1 Syngeneic



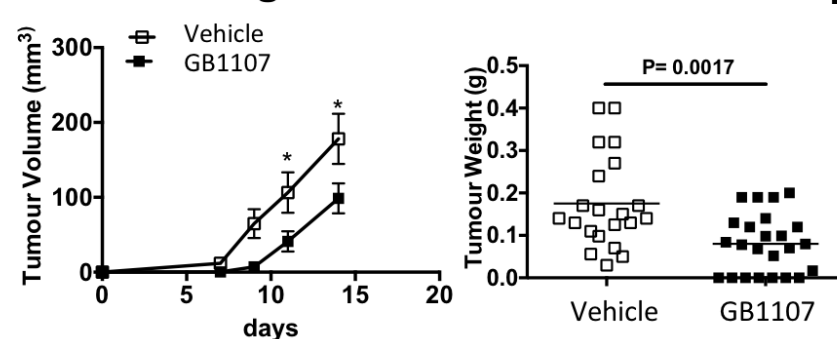
C: LLC1 lung colonization



D



E: Human galectin-3 KI host



F: Galectin-3:WB

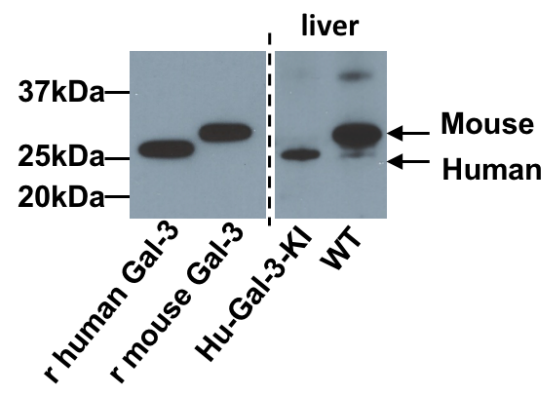


Figure 4

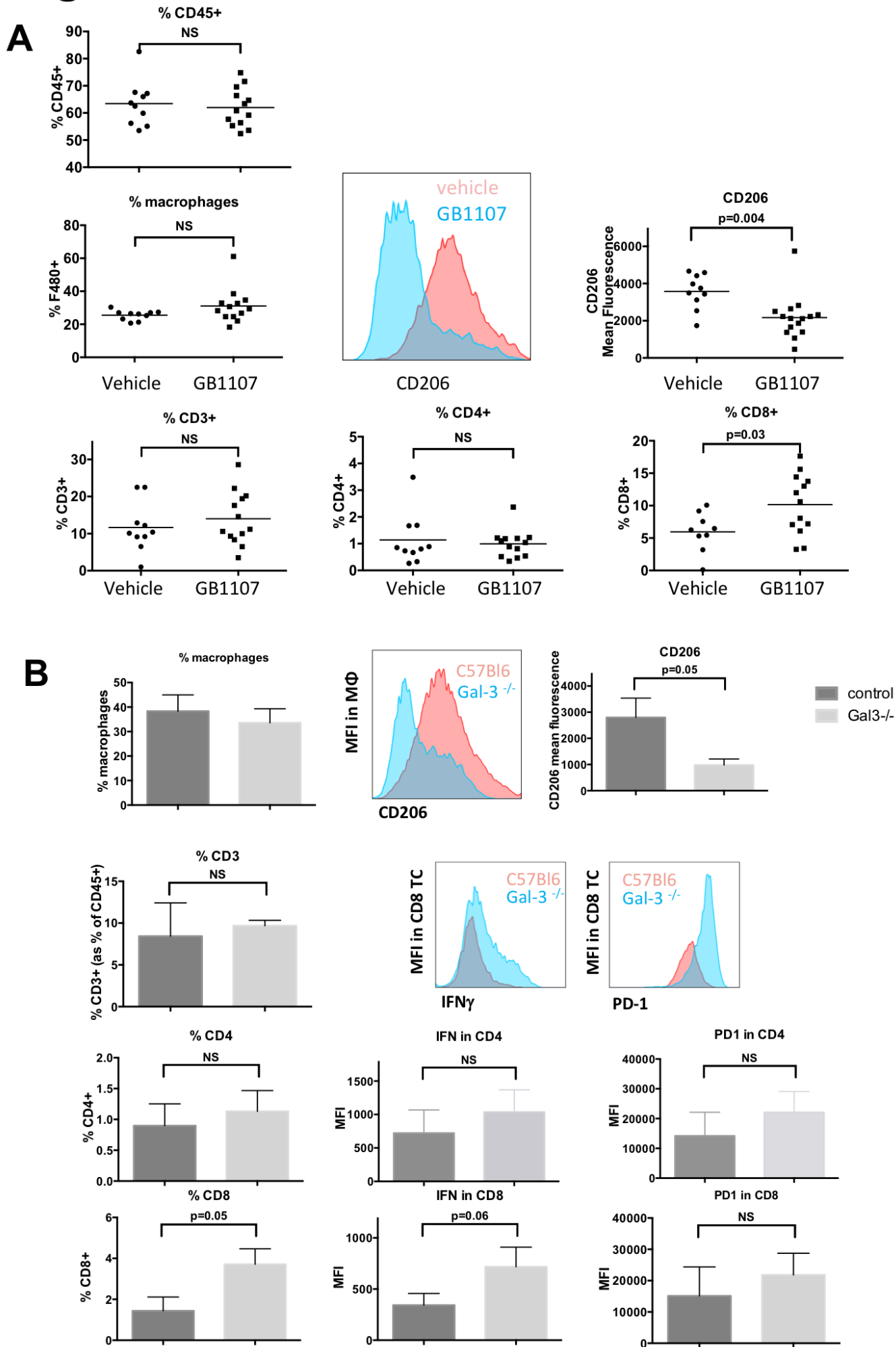


Figure 5

